International Journal of Mass Spectrometry 297 (2010) 76–84

Contents lists available at ScienceDirect

International Journal of Mass Spectrometry

journal homepage: www.elsevier.com/locate/ijms

The sodium cation-bound dimer of theophylline: IRMPD spectroscopy of a highly symmetric electrostatically bound species

Richard A. Marta*, Ronghu Wu, Kris R. Eldridge, Jonathan K. Martens, Terry B. McMahon**

Department of Chemistry, University of Waterloo, Waterloo, Ontario, Canada N2L 3G1

ARTICLE INFO

Article history:
Received 10 April 2010
Received in revised form 18 June 2010
Accepted 22 June 2010
Available online 26 June 2010

Keywords:
Infrared multiphoton dissociation
Sodium cation-bound adducts
Gaseous ion energetics and structure

ABSTRACT

Sodium cation-carbonyl interactions resulting from the formation of a sodium cation-bound dimer (SCBD) of a common bronchodilator, theophylline have been probed using infrared multiple photon dissociation (IRMPD) spectroscopy and electronic structure calculations. Energies have been determined at the MP2(full)/aug-cc-pCVTZ//B3LYP/6-311+G(d,p) level of protocol for all heteroatoms involved in sodium interactions, including sodium and at the MP2(full)/6-311+G(2d,2p)//B3LYP/6-311+G(d,p) level of protocol for all remaining heavy and hydrogen atoms. Six stable isomers of the SCBD of theophylline have been proposed within a range of relative Gibbs free energies of ~36 kJ mol^{-1} (298 K). The most favourable isomer (10.9 kJ mol^{-1} over the next isomer at 298 K) exhibits an average zero net dipole moment due to free rotation of theophylline molecules about a C═O···Na$^+$···O═C axis, facilitated by the relatively large interatomic distance (4.28 Å) between the carbonyl oxygen atoms. This is also shown to effectively isolate the theophylline molecules from interaction resulting in a significant reduction in the observed vibrational anharmonicity. Such a feature provides a chemical system that can be more suitably simulated by a spectrum calculated using a harmonic, rather than anharmonic oscillator approximation. This is important since the system described here is 37 times more costly to produce using an anharmonic oscillator approximation relative to the analogous harmonic calculation at the B3LYP/6-311+G(d,p) level of protocol with the same computational resources. Accurate characterization of both the free and sodiated carbonyl stretches, as well as several other frequencies of the SCBD of theophylline gives insight into cation–molecule interactions and also provides a useful contribution to the growing database of gas phase infrared spectral assignments.

1. Introduction

Theophylline has been used therapeutically in asthma sufferers for the last 70 years due to its bronchodilator properties. Specifically, theophylline acts as an inhibitor of the enzyme phosphodiesterase (PDE), resulting in an increase in the availability of cyclic adenosine monophosphate (cAMP) and therefore relaxing the smooth muscle of the airway [1].

Theophylline-associated seizures (TAS) have been observed as a neurological emergency in children both with and without epilepsy who were exposed to only therapeutic levels of theophylline. The mechanism of TAS has been investigated recently by Fukuda et al. [2] using experiments involving hyperthermia-induced seizures in juvenile rats following exposure to theophylline under varying conditions. Fukuda et al. report that addition of a selective adenosine A_1 agonist in conjunction with an adenosine kinase inhibitor nullifies the onset of TAS, suggesting that blockage of the adenosine A_1 receptor by theophylline is the main cause of TAS.

There has also been research into the development of RNA aptamer-based electrochemical sensors for sensitive, selective and label-free detection of theophylline in serum [3]. The sensor is described to selectively differentiate theophylline from structurally similar caffeine and theobromine; however, reliable performance of the sensor in dilute solutions of serum has been elusive.

Recently, we have been exploring functionality of methylxanthines such as caffeine and theophylline by probing the structures of electrosprayed gaseous ions using the powerful technique of infrared multiple photon dissociation (IRMPD) spectroscopy, coupled with electronic structure calculations [4]. Structures of both protonated caffeine and theophylline, as well as the proton-bound dimer (PBD) of ammonia and theophylline have been determined accurately and unambiguously using this technique. The work has provided insight into differences in functionality between theophylline and caffeine. For example, proton-transport catalysis (PTC) results in complication of the IRMPD spectrum of protonated theophylline compared to that of protonated caffeine. The proton-

* Corresponding author. Tel.: +1 519 888 4576x36388.
** Corresponding author. Tel.: +1 519 888 4576x84591.
E-mail addresses: ramarta@uwaterloo.ca (R.A. Marta), mcmahon@uwaterloo.ca (T.B. McMahon).

1387-3806/$ – see front matter © 2010 Elsevier B.V. All rights reserved.
doi:10.1016/j.ijms.2010.06.021

bound dimer of theophylline is observed to contain a particularly stable bidentate ionic hydrogen bond (IHB) which cannot be formed analogously by caffeine. Both of the preceding examples demonstrate that small differences in structure between caffeine and theophylline can result in significant differences in their functionality and reactivity. Finally, consideration of anharmonicity has been shown [4] to be essential for simulating the spectra of the protonated systems described above, especially in the case of the PBD of theophylline and ammonia, where multiply coupled vibrations exist predominantly due to short-range electrostatic interactions.

Methylxanthines contain two chemically distinct carbonyl groups, thus interaction with either carbonyl oxygen results in a distinct shift in frequency of the infrared absorption of the carbon–oxygen bond. Such shifts in frequency can be observed using mass-selected IRMPD spectroscopy in the spectral range of 1000–1900 cm^{-1} and simulated using electronic structure calculations. Other diagnostic vibrational modes can be observed and assigned confidently only if the experimental spectrum is sufficiently well resolved; however, carbonyl groups generally exhibit intense absorption bands and it is because of this that their spectral assignments are generally the most reliable. Because the carbonyl oxygen atoms of methylxanthines, such as theophylline, are rich in electrons they can be expected to engage in several types of interactions with electophilic species. Sodium cation (Na^+) presents an interesting, and biologically relevant, ion with which to investigate alkali metal cation-molecule interactions with theophylline.

There has been substantial research in the area of gas phase metal cation–molecule interactions over the last decade including studies involving the structural elucidation of metal cationized-molecules by IRMPD spectroscopy [5–27], in addition to measurements of sodium cation affinities (SCAs) [28–44].

One study has compared the IRMPD spectra of sodium cationized glycine (Gly) and proline (Pro), in order to determine if such interactions would lead to charge-solvated (CS) or salt-bridged (SB) structures [13]. This work has shown both spectroscopically and computationally that Gly–Na^+ is likely to favour a charge-solvated structural configuration, while Pro–Na^+ favours a salt-bridged structural configuration. Similarly, Carl et al. [10] have conclusively shown that charge-solvated conformations are favoured upon the formation of tridentate interactions between alkali metal cations (Li^+, Na^+, K^+, Rb^+ and Cs^+) and the amine nitrogen, carbonyl oxygen and sulphur atoms contained in methionine (Met). Prell et al. [14] have demonstrated, using very high quality IRMPD spectra and electronic structure calculations, that trivalent lanthanide metals cations La^{3+}, Ho^{3+} and Eu^{3+} form a SB with Ala_n (n = 2–5) in which all of the carbonyl groups solvate the metal cation. They have also shown that the IRMPD spectra of Leu-enk (Tyr-Gly-Gly-Phe-Leu) coordinated with the same trivalent metal cations exhibit strong free carbonyl stretching signatures, suggesting that side chain behaviour of tyrosine (Tyr) and phenylalanine (Phe) may interfere with complete coordination of the cation by the carbonyls.

Wang et al. [31] obtained the SCAs of systems involving interactions of sodium cation with cytosine and methyl cytosine derivatives using kinetic methods and electronic structure calculations. Similarly, Armentrout et al. [45] have rigorously extracted alkali metal cation affinities and structural data for methionine (Met) including Met–Li^+, Met–Na^+ and Met–K^+ using threshold collision-induced dissociation with xenon in a guided ion beam mass spectrometer and high-level electronic structure calculations.

Although many excellent IRMPD studies have yielded detailed descriptions of alkali metal cation interactions with amino acids and peptides [6–9,11,13,14,46], methylxanthines demonstrate another unexplored example of small biologically relevant molecules possessing the necessary attributes amenable to IRMPD spectroscopy experiments in the spectral region of 1000–1900 cm^{-1}. Here the IRMPD spectrum of the sodium cation-bound dimer (SCBD) of theophylline is presented; in compliment to recent work showing the IRMPD spectra of both protonated theophylline and the PBD of theophylline and ammonia [4].

2. Experimental

The IRMPD experiments have been performed using the infrared free electron laser (IR-FEL) at the Centre de Laser Infrarouge d'Orsay (CLIO) facility in Orsay, France. The IR-FEL beam was guided into a Bruker Esquire 3000+ ion trap mass spectrometer, equipped with electrospray ionization. This experimental arrangement has previously been described in detail [47–49]. The IR-FEL beam was produced by emission from a 10-50 MeV electron beam, and the emission photon wavelength can be tuned, through the mid-infrared range, by adjusting the physical gap between a set of periodic undulator magnets. The undulator is housed within a 4.8 m long optical cavity. The laser beam is accumulated in the optical cavity and outcoupling is permitted through a 1–3 mm hole in one of two silver mirrors, each with a diameter of 38 mm.

The present work used an electron energy of 48 MeV which permitted continuous scans over a range of 1000–2000 cm^{-1}. The IR-FEL output consists of a train of 8 μs macropulses, with a repetition rate of 25 Hz. Each macropulse is comprised of approximately 500 micropulses, with a width of a few picoseconds per pulse. For an average IR power of 500 mW, the corresponding micropulse and macropulse energies are about 40 μJ and 20 mJ, respectively.

Solutions of sodium cation and theophylline were prepared by combining a 2:1 mixture of sodium chloride and theophylline, respectively (~10 μM). The solvent system consisted of a 1:1 mixture of acetonitrile and water. Ions were provided from the solution using electrospray ionization. The desired ionic species was isolated and confined within the ion trap where it then experienced multiple collisions with Helium buffer gas (~1 mTorr) for 40 ms prior to irradiation by the IR-FEL. The IR-FEL beam was then focused and introduced into the center of the ion trap of the mass spectrometer. Consequence mass spectra were recorded following a laser irradiation time of 150 ms, with an accumulation of ten spectra obtained for each wavelength. IRMPD spectra were acquired by scanning the wavelength in steps of ~4 cm^{-1}, with the IR-FEL power fluctuating by an average of ±15% over an experimental range of 1000–1850 cm^{-1}. The single spectrum reported here is expressed in terms of the fragmentation efficiency, P_{frag}, as a function of the photon energy, in cm^{-1}. Where I_{parent} and $\Sigma I_{fragment}$ are the parent and sum of the fragment ion intensities, respectively.

$$P_{frag} = -\log\left[\frac{I_{parent}}{I_{parent} + \sum I_{fragment}}\right] \quad (1)$$

2.1. Electronic structure calculations

Electronic structure calculations have been performed using the Gaussian 09 software package [50]. All proposed isomers of the SCBD of theophylline were optimized using density functional theory (DFT), employing the B3LYP exchange–correlation functional and the 6-311+G(d,p) basis set. B3LYP is known to be a relatively reliable and economical computational method and is extensively employed in the investigation of small and medium size molecules [49,51–56]. All harmonic frequencies obtained at this level of theory were scaled by 0.9679 [57] in order to compensate for errors arising from the use of a harmonic oscillator approximation in calculating the frequencies, as well as, long range electron correlation effects. Anharmonic frequencies [50,58] have also been obtained at the B3LYP/6-311+G(d,p) level of theory for only the most chemically significant species.

It is well established that hybrid DFT methods such as B3LYP generally outperform local or gradient-corrected DFT, and MP2

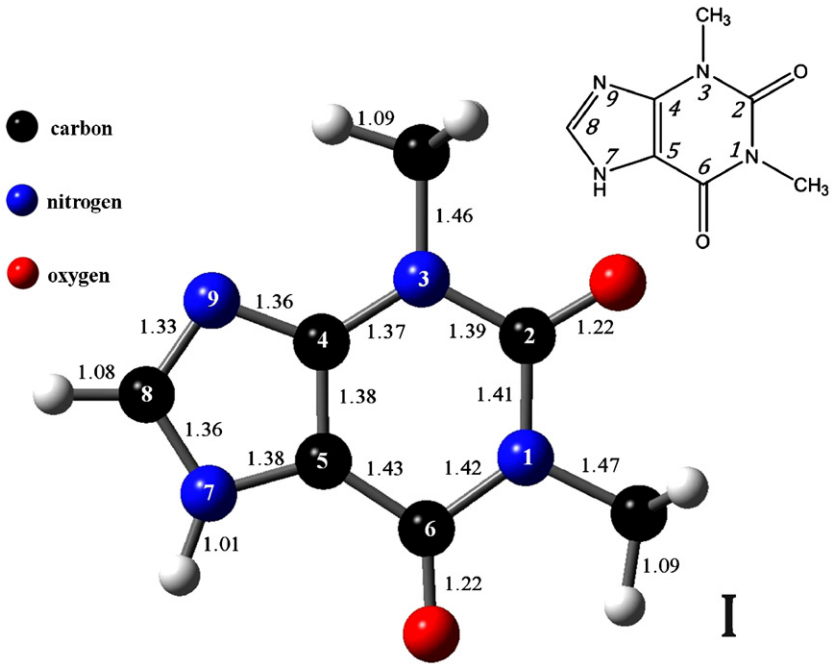

Fig. 1. Calculated structure of theophylline (**I**), with bond lengths in Angstroms (Å) and optimized at the B3LYP/6-311+G(d,p) level of protocol. A numbered "stick structure" of theophylline is provided in the top right corner for additional clarity.

for the prediction of fundamental frequencies and their associated infrared intensities [7,13,56,59–66]. Fundamental frequencies calculated by the MP2 method are significantly more costly and sometimes less accurate than those produced by B3LYP, thus, all geometry optimizations and calculated frequencies reported here have been obtained using the B3LYP method. In order to provide more realistic simulated spectra, calculated line spectra have been fit using Lorentzian functions with full-width at half maximum (FWHM) of 15 cm^{-1} specified.

All optimized structures have been verified as minima by performing frequency calculations, in order to ensure that no imaginary frequencies were present. Geometry optimizations produced with Gaussian 09 [50] have been calculated with "tight" force, displacement (opt = tight) and energy convergence (scf = tight) specified. Single point energy calculations have been obtained with the condition of "tight" energy convergence (scf = tight) specified. In order to ensure that no significant differences exist between B3LYP and MP2 obtained geometries, a selection of B3LYP/6-311+G(d,p) level geometries have been optimized and verified by frequency calculations as local minima at the MP2/6-311+G(d,p) protocol. The mean absolute deviation (MAD) between calculated bond lengths at the B3LYP and MP2/6-311+G(d,p) level of theory reported here is found to be only 0.017 pm, or 0.45% of the average bond length of the optimized structures.

In order to provide more accurate energies for the SCBD systems, single point calculations have been specified at the MP2(full)/aug-cc-pCVTZ level of theory for sodium and all heavy atoms involved in interactions with sodium cation, with all of the remaining heavy and hydrogen atoms specified at the MP2(full)/6-311+G(2d,2p) level of protocol. The notation for the protocol described previously will now continue to be defined as, MP2(full)/aug-cc-pCVTZ[Na,N(9),O(2),O(6)]/6-311+(2d,2p). It has been suggested that calculations involving sodium cation should include core–core and core–valence electron correlation [45,67,68] and the aug-cc-pCVTZ basis set [69,70] has been optimized for use with methods that include core–core and core–valence correlation, such as MP2(full). The validity of the level of protocol described above for calculating single point energies of the systems presented here has been evaluated by calculating energies of the sodiated theophylline isomers using single point calculations at the MP2(full)/aug-cc-pCVTZ level of protocol. It is not yet possible to verify this for the dimers with the currently available computing resources. Calculation of the SCAs of three sodiated theophylline isomers has shown that minimal differences exist between the calculated free energies of sodiation (298 K) using the different levels of protocol described above, with a MAD of only 0.21 kJ mol^{-1}.

3. Discussion

The calculated structure of theophylline (**I**) is shown in Fig. 1 and the three most favourable sites of protonation [4] with respect to free energy (298 K) as N(9), O(2) and O(6). The cyclic amide nitrogen atoms, N(1) and N(3) are not Lewis basic due to the fact that their lone pairs are highly delocalized about the ring system and carbonyl oxygen atoms. All four isomers afforded by protonation occurring at the N(1) or N(3) site have previously been shown to be thermally inaccessible under the experimental conditions described here [4].

It is found that Na^+ does not form stable interactions with either N(1) or N(3) in theophylline at the B3LYP/6-311+G(d,p) level of protocol and as such, only sodiated monomers with Na^+ interacting at N(9), O(2) and O(6) will be considered (Fig. 2). Sodium cation–π interactions [35,37–40] have also been considered, but have been found to be unfavourable in this system. The SCAs, entropies and free energies of sodiation (298 K) have been calculated for the N(9), O(2) and O(6) positions and are shown in Table 1. Sodiation of the N(9) site is significantly higher in free energy (298 K) than at O(2) or O(6) and thus, it should be reasonable to exclude the existence of isomer $\mathbf{II}_{N(9)}$ under the experimental conditions. Interestingly, it has been shown both experimentally and theoretically that protonation of theophylline is favoured at N(9) followed by O(2) and O(6), respectively [4]. Upon sodiation of theophylline, calculations predict a minor contraction of the free carbonyl bond length by 0.01 Å in all three proposed isomers (Fig. 2). For isomers $\mathbf{III}_{O(6)}$ and $\mathbf{IV}_{O(2)}$, it is predicted that extensions of the $Na^+\cdots$carbonyl bond lengths will occur by 0.04 and 0.03 Å, respectively. Not surprisingly, the highest energy isomer ($\mathbf{II}_{N(9)}$) exhibits the longest $Na^+\cdots$(heteroatom)

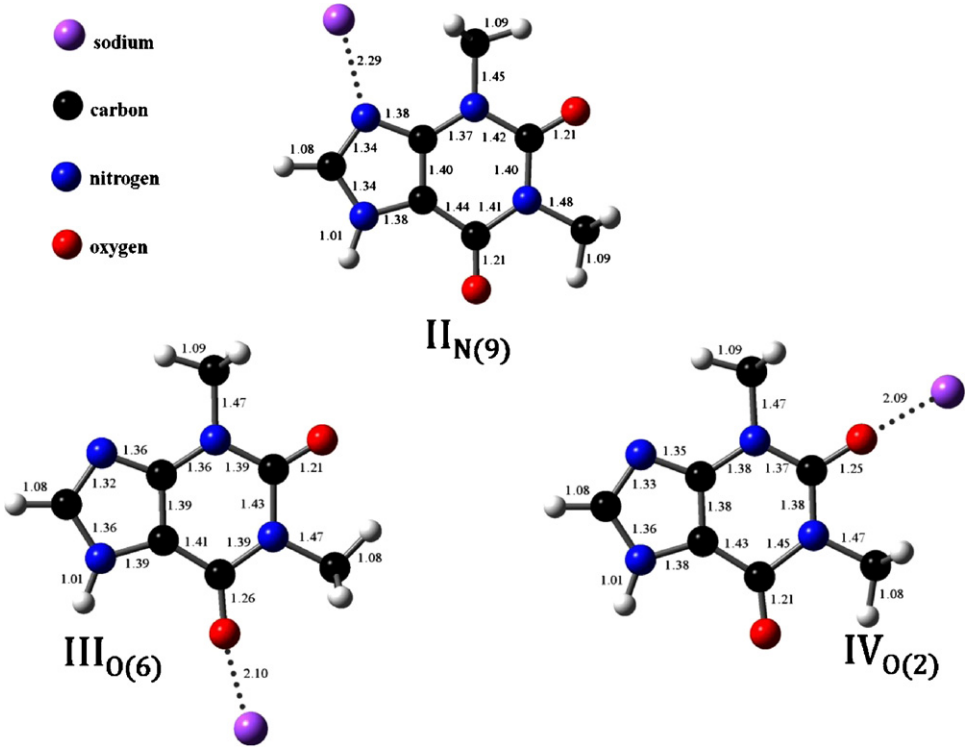

Fig. 2. Calculated stable structures of sodiated theophylline, with bond lengths in Angstroms (Å) and optimized at the B3LYP/6-311+G(d,p) level of protocol.

Table 1
Calculated SCAs and thermodynamic quantities associated with the sodiation of theophylline (Fig. 2). Energies have been calculated at the MP2(full)/aug-cc-pCVTZ[Na,N(9),O(2),O(6)]/6-311+(2d,2p)//B3LYP/6-311+G(d,p) level of protocol. The energies in parentheses are calculated strictly at the MP2(full)/aug-cc-pCVTZ//B3LYP/6-311+G(d,p) level of protocol. All energies are reported in units of kJ mol^{-1} and calculated at 298 K.

Species	SCA ($-\Delta H_{298}^{\circ}$)	$-\Delta S_{298}^{\circ}$	$-\Delta G_{298}^{\circ}$	$\Delta\Delta G_{298}^{\circ}$
$\mathbf{II}_{N(9)}$	114 (111)	−102	−83.8 (−80.7)	38.6 (38.5)
$\mathbf{III}_{O(6)}$	142 (139)	−96.2	−113 (−110)	9.10 (8.78)
$\mathbf{IV}_{O(2)}$	153 (150)	−104	−122 (−119)	0.00 (0.00)

interaction distance of 2.29 Å, followed by 2.10 and 2.09 Å for isomers $\mathbf{III}_{O(6)}$ and $\mathbf{IV}_{O(2)}$, respectively.

Six stable isomers of the SCBD of theophylline have been proposed, with their calculated structures shown in Fig. 3 and thermodynamic values in Table 2. Calculations find it more unfavourable for Na^+ to associate with N(9), relative to O(2) and O(6). This is most pronounced in the asymmetric dimers $\mathbf{VI}_{O(6)/N(9)}$ and $\mathbf{VII}_{O(2)/N(9)}$, both of which exhibit the weakest binding energies, followed by the symmetric dimer $\mathbf{V}_{N(9)/N(9)}$. Based on relative free energies (298 K), the SCBD of theophylline should exist predominantly as isomer $\mathbf{X}_{O(2)/O(2)}$, with the efficient sharing of Na^+ characterized by a symmetric bond about the C(2)═O···Na^+···O═C(2) axis (Table 2). The relatively large distance between the oxygen atoms of 4.28 Å facilitates free rotation about the C(2)═O···Na^+···O═C(2) axis. By scanning the rotation of one of the theophylline substituents about the C(2)═O···Na^+···O═C(2) axis into the fully eclipsed configuration, the electronic energy increases by an insubstantial 0.1 kJ mol^{-1}. The chemical significance of the electrostatic interaction resulting in free rotation of the theophylline substituents, is that isomer $\mathbf{X}_{O(2)/O(2)}$ will possess an average net zero dipole moment. Although isomer $\mathbf{X}_{O(2)/O(2)}$ is considered to be the dominant species, the existence of spectral contributions from isomers $\mathbf{VIII}_{O(6)/O(6)}$ and $\mathbf{IX}_{O(2)/O(6)}$ in the IRMPD spectrum should not be neglected since their calculated free energies relative to $\mathbf{X}_{O(2)/O(2)}$ are only 11.6 and 10.9 kJ mol^{-1}, respectively. A detailed image of the optimized structure of isomer $\mathbf{X}_{O(2)/O(2)}$ is depicted in Fig. 4.

Table 2
Calculated thermodynamic quantities associated with the proposed SCBDs of theophylline (Fig. 3). Energies have been calculated at the MP2(full)/aug-cc-pCVTZ[Na,N(9),O(2),O(6)]/6-311+(2d,2p)//B3LYP/6-311+G(d,p) level of protocol. All energies are reported in units of kJ mol^{-1} and calculated at 298 K.

Species	ΔH_{298}°	ΔS_{298}°	ΔG_{298}°	$\Delta\Delta G_{298}^{\circ}$
$\mathbf{V}_{N(9)/N(9)}$	−96.3	−123	−59.6	31.0
$\mathbf{VI}_{O(6)/N(9)}$	−90.4	−119	−54.8	35.8
$\mathbf{VII}_{O(2)/N(9)}$	−90.1	−114	−56.1	34.5
$\mathbf{VIII}_{O(6)/O(6)}$	−113	−113	−79.1	11.6
$\mathbf{IX}_{O(2)/O(6)}$	−112	−108	−79.8	10.9
$\mathbf{X}_{O(2)/O(2)}$	−122	−106	−90.6	0.00

The gas phase IR action spectrum of the SCBD of theophylline has been obtained by mass-isolating the ion at m/z 383 and performing IRMPD to afford sodiated theophylline at m/z 203. The intensities of both precursor and product ion have been used with Eq. (1) as a function of FEL photon energy to produce a high quality IRMPD spectrum clearly showing several diagnostic modes. The IRMPD spectrum of the SCBD of theophylline and calculated harmonic spectra of the three most favourable isomers, including an anharmonic spectrum of isomer $\mathbf{X}_{O(2)/O(2)}$, are shown in Fig. 5 with spectral assignments available in Table 3. Although isomer $\mathbf{VII}_{O(2)/N(9)}$ is significantly higher in free energy (298 K) than isomers $\mathbf{VIII}_{O(6)/O(6)}$, $\mathbf{IX}_{O(2)/O(6)}$ and $\mathbf{X}_{O(2)/O(2)}$, its spectrum is also included in Fig. 5 demonstrating calculated vibrational signatures of a dimer possessing an inefficient sharing of Na^+,

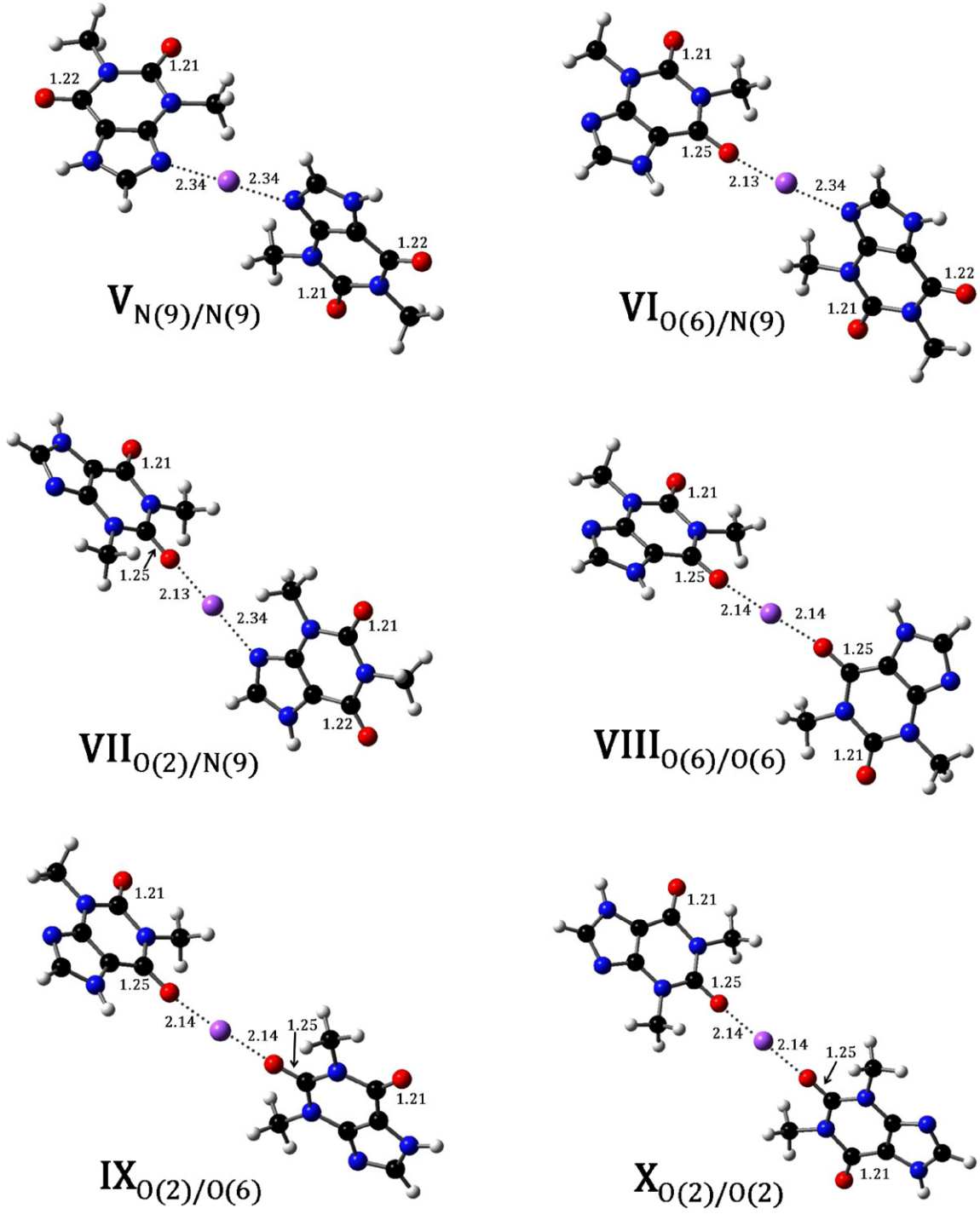

Fig. 3. Calculated stable structures of the SCBD of theophylline, with bond lengths in Angstroms (Å) and optimized at the B3LYP/6-311+G(d,p) level of protocol.

specifically engaged in a C(2)═O···Na^+···N(9) interaction between the theophylline molecules. The IRMPD spectrum of the SCBD of theophylline exhibits vibrational signatures indicative of exclusively C═O···Na^+···O═C interactions. The spectral feature predicted to occur at 1743 cm^{-1} according to the calculated spectrum of isomer **VII**$_{O(2)/N(9)}$, but absent from the IRMPD spectrum, arises from the asymmetric stretches (ν_{as}) of two free carbonyls located at C(2) and C(6) of one of the theophylline molecules. Based on the calculated relative free energy (298 K) of isomer **VII**$_{O(2)/N(9)}$ and the IRMPD spectrum of the SCBD of theophylline, it is reasonable to assume that no appreciable quantity of a C(2)═O···Na^+···N(9) interacting isomer exists under the experimental conditions.

The first prominent signature observed in the IRMPD spectrum is located at 1758 cm^{-1} and is associated with the symmetric (ν_s) and asymmetric (ν_{as}) free carbonyl stretches of C(2)═O and C(6)═O, with the dominant contribution arising from the more intense asymmetric mode. Our previous work [4] has shown the free carbonyl stretch of the PBD of theophylline and ammonia to exist at 1757 cm^{-1} in the IRMPD spectrum, supporting the spectral assignment proposed here. In all three of the lowest energy isomers (**VIII**$_{O(6)/O(6)}$, **IX**$_{O(2)/O(6)}$ and **X**$_{O(2)/O(2)}$) the free C(2)═O and C(6)═O stretches are located consistently at 1776 and 1782 cm^{-1}, respectively, with the calculated harmonic values lying blue-shifted of the experimental peak. Anharmonic calculation of the spectrum of iso-

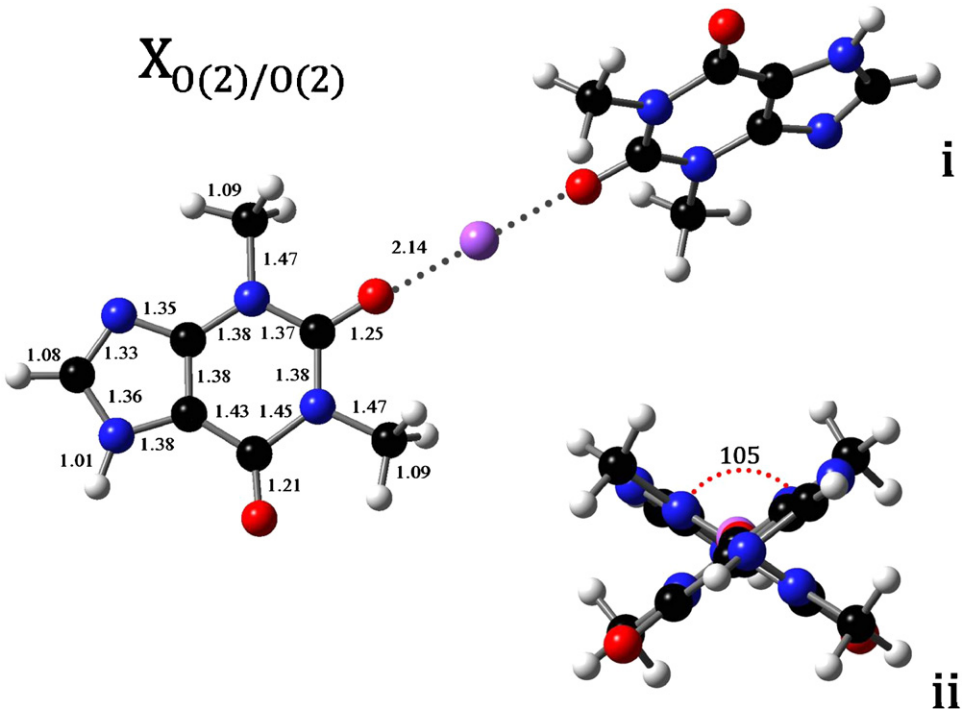

Fig. 4. (i) Calculated structure of isomer $\mathbf{X}_{O(2)/O(2)}$ of the SCBD of theophylline, with bond lengths in Angstroms (Å) and optimized at the B3LYP/6-311+G(d,p) level of protocol, with half of the ion labelled since it possesses exact bond symmetry in each of the theophylline substituents. (ii) A view of the dihedral angle (in degrees) formed by looking down the C(2)═O···Na^+···O═C(2) axis.

mer $\mathbf{X}_{O(2)/O(2)}$ places the mode at 1744 cm^{-1}, which is red-shifted relative to the experimental peak, suggesting that neither the harmonic or anharmonic oscillator approximations are able to closely simulate this particular mode at the B3LYP/6-311+G(d,p) level of protocol. Another visibly dominant peak in the IRMPD spectrum is located at 1646 cm^{-1} and can be attributed to a strong asymmetric carbonyl stretch associated with C═O···Na^+ interaction. The vibrational signatures through the spectral range of 1600–1650 cm^{-1} are rather broadened; however, the IRMPD spectrum shows what could be described as a small shoulder located at 1625 cm^{-1}, which can be ascribed to a weak asymmetric carbonyl stretch associated with C═O···Na^+ interaction. The calculated harmonic values

Table 3
Infrared peak assignments associated with the IRMPD and calculated spectra for the SCBD of theophylline presented in Fig. 5. A subscript on a carbon atom indicates which theophylline molecule the mode is associated with. The value in parentheses next to a carbon atom indicates the atom number. Photon energies and MADs from the IRMPD photon energies are reported in units of cm^{-1}. Values shown in parentheses next to photon energies are calculated intensities in units of km mol^{-1}.

Mode	IRMPD	$\mathbf{X}_{O(2)/O(2)}$ (harmonic)	$\mathbf{X}_{O(2)/O(2)}$ (anharmonic)	$\mathbf{IX}_{O(2)/O(6)}$	$\mathbf{VIII}_{O(6)/O(6)}$
$\nu_{as}(C_1(2)═O···Na^+ + C_2(2)═O···Na^+) + \nu_s(C_{1/2}(2)═O···Na^+ + C_{1/2}(6)═O)$	1758	1782 (792)	1744	–	–
$\nu_s(C_1(2)═O···Na^+ + C_2(2)═O···Na^+) + \nu_s(C_{1/2}(2)═O···Na^+ + C_{1/2}(6)═O)$		1782 (441)	1744	–	–
$\nu_{as}(C_1(6)═O···Na^+ + C_2(6)═O···Na^+) + \nu_s(C_{1/2}(6)═O···Na^+ + C_{1/2}(2)═O)$		–	–	–	1776 (688)
$\nu_{as}(C_1(2)═O + C_2(2)═O)$		–	–	–	1776 (391)
$\nu_s(C_1(6)═O + C_1(2)═O···Na^+)$		–	–	1782 (618)	–
$\nu_s(C_2(2)═O + C_2(6)═O···Na^+)$		–	–	1776 (539)	–
$\nu_{as}(C_1(6)═O···Na^+ + C_2(6)═O···Na^+) + \nu_{as}(C_{1/2}(6)═O···Na^+ + C_{1/2}(2)═O)$	1646	–	–	–	1672 (2297)
$\nu_s(C_1(6)═O···Na^+ + C_2(6)═O···Na^+) + \nu_{as}(C_{1/2}(6)═O···Na^+ + C_{1/2}(2)═O)$	1625	–	–	–	1687 (13)
$\nu_{as}(C_1(2)═O···Na^+ + C_2(6)═O···Na^+) + \nu_{as}(C_{1/2}(2/6)═O···Na^+ + C_{1/2}(6/2)═O)$		–	–	1660 (1554)	–
$\nu_{as}(C_1(2)═O···Na^+ + C_1(6)═O)$		–	–	1629 (179)	–
$\nu_{as}(C_2(6)═O···Na^+ + C_1(2)═O)$		–	–	1623 (189)	–
$\nu_{as}(C_1(2)═O···Na^+ + C_2(2)═O···Na^+) + \nu_{as}(C_{1/2}(2)═O···Na^+ + C_{1/2}(6)═O)$		1656 (1658)	1620	–	–
		1628 (384)	1592	–	–
$\rho_s(N(7)–H + C(8)–H) + \delta_s(CH_3)$	1568	1578 (205)	1534	1578 (187)	1577 (283)
	1250	1256 (58)	1231	1263 (51)	1263 (84)
	1435	1429 (287)	1387	1430 (147)	1429 (158)
ν_{ring}	1363	1364 (37)	1326	1364 (28)	1354 (24)
$\rho(C(8)–H) + \delta_s(CH_3)$	1220	1217 (87)	1190	1223 (31)	1222 (46)
$\rho_{as}(N(7)–H) + C(8)–H$	1096	1114 (70)	1088	1122 (15)	1122 (19)
$\rho(CH_3)$	1061	1060 (98)	1036	1061 (49)	1053 (34)
MAD from IRMPD	0	11	28	10	22

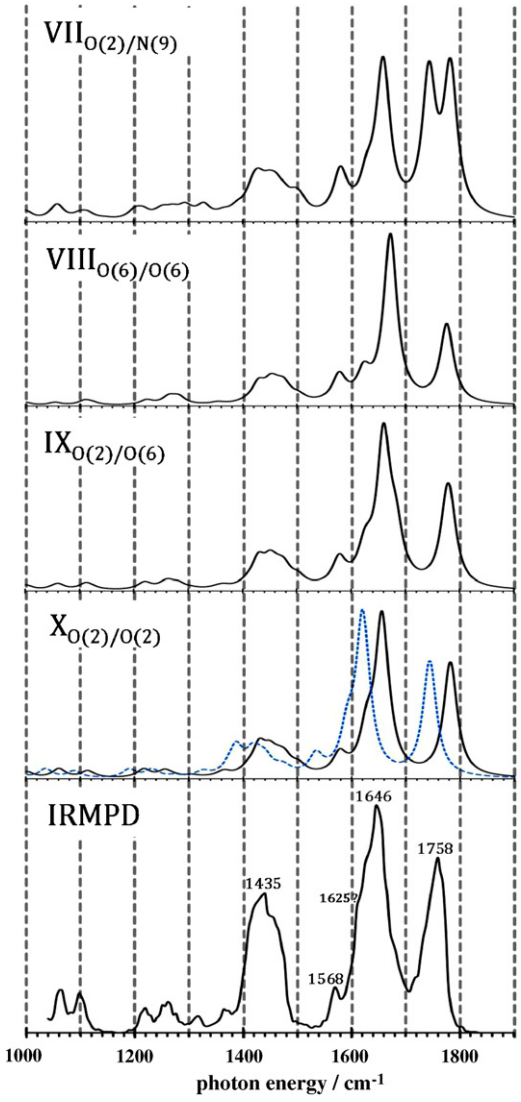

Fig. 5. IRMPD spectrum of the SCBD of theophylline (bottom) and the calculated harmonic spectra of three of the lowest energy isomers ($\mathbf{X}_{O(2)/O(2)}$, $\mathbf{IX}_{O(2)/O(6)}$ and $\mathbf{VIII}_{O(6)/O(6)}$) determined at the B3LYP/6-311+G(d,p) level of protocol (scaled by 0.9679). The calculated anharmonic spectrum of $\mathbf{X}_{O(2)/O(2)}$ is indicated by a blue-coloured dashed line. The calculated harmonic spectrum of isomer $\mathbf{VII}_{O(2)/N(9)}$ is included to demonstrate vibrational signatures of a C(2)═O···Na$^+$···N(9) interaction. Intensities for the experimental and calculated spectra are in relative units of IRMPD efficiency and km mol^{-1}, respectively.

of the subsequently described modes for isomer $\mathbf{X}_{O(2)/O(2)}$ are predicted to occur at 1656 and 1628 cm^{-1}, respectively, and are in good agreement with experiment. This is followed closely by the second most favourable isomer, $\mathbf{IX}_{O(2)/O(6)}$, with calculated harmonic values located at 1660 and 1629 cm^{-1}, respectively. Finally, isomer $\mathbf{VIII}_{O(6)/O(6)}$ has two calculated harmonic values attributed to asymmetric and symmetric Na$^+$···O═C stretches located at 1687 and 1672 cm^{-1}, respectively, showing less evidence to support the existence of isomer $\mathbf{VIII}_{O(6)/O(6)}$ under the experimental conditions. Calculated anharmonic values for the peaks located at 1646 and 1625 cm^{-1} in the IRMPD spectrum for isomer $\mathbf{X}_{O(2)/O(2)}$ are 1620 and 1592 cm^{-1}, respectively, again demonstrating a red-shift from experiment.

There are several other spectral assignments detailed in Table 3 and shown by Fig. 5 suggesting that $\mathbf{IX}_{O(2)/O(6)}$ and $\mathbf{X}_{O(2)/O(2)}$ are the dominant isomers displayed in the IRMPD spectrum, which is also consistent with the predicted relative free energies (298 K)

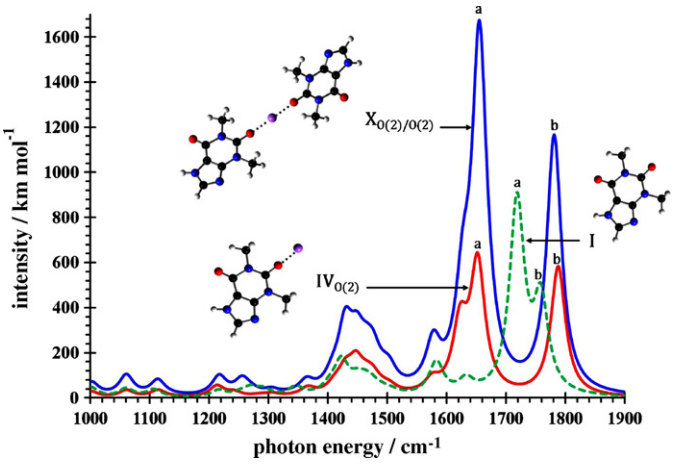

Fig. 6. The calculated harmonic spectra of theophylline (**I** – dashed green), sodiated theophylline ($\mathbf{IV}_{O(2)}$ – solid red) and the SCBD of theophylline ($\mathbf{X}_{O(2)/O(2)}$ – solid blue) determined at the B3LYP/6-311+G(d,p) level of protocol (scaled by 0.9679). The labels a and b show the frequency shifts of the theophylline C═O stretching modes upon sodiation.

obtained by electronic structure calculations (Table 2). Although calculated IR intensities will not be compared here to IRMPD intensities due to the complex nature of the IRMPD process, the match between the calculated harmonic frequencies of both isomers $\mathbf{IX}_{O(2)/O(6)}$ and $\mathbf{X}_{O(2)/O(2)}$ with the IRMPD spectrum of the SCBD of theophylline is very good, with a MAD of only 10 and 11 cm^{-1}, respectively. If the ions are assumed to be thermalized by sufficient collisions with helium buffer gas and cannot readily isomerize during the IRMPD process, then calculations of the free energies of SCBD formation (298 K) predict the distribution of isomers $\mathbf{IX}_{O(2)/O(6)}$ and $\mathbf{X}_{O(2)/O(2)}$ to exist as approximately 1–81. If the IRMPD efficiencies of the isomers are assumed to be equivalent, then $\mathbf{X}_{O(2)/O(2)}$ should be the dominant isomer shown by the IRMPD spectrum of the SCBD of theophylline.

A particularly interesting feature of the calculated harmonic spectrum of $\mathbf{X}_{O(2)/O(2)}$ is its resemblance to that of sodiated monomer $\mathbf{IV}_{O(2)}$ (Fig. 6). Bond lengths of theophylline bound to Na$^+$ in $\mathbf{IV}_{O(2)}$ are identical to those found in both of the theophylline molecules bound to Na$^+$ in $\mathbf{X}_{O(2)/O(2)}$, with the only exception being a difference in the distance of the C(2)═O···Na$^+$ electrostatic interactions. The length of the C(2)═O···Na$^+$ interactions in $\mathbf{IV}_{O(2)}$ and $\mathbf{X}_{O(2)/O(2)}$ are 2.10 and 2.13 Å, respectively. The calculated harmonic frequencies of the C═O stretching modes a and b are 1759 and 1719 cm^{-1} for theophylline, 1788 and 1653 cm^{-1} for $\mathbf{IV}_{O(2)}$ and 1782 and 1656 cm^{-1} for $\mathbf{X}_{O(2)/O(2)}$, respectively (Fig. 6). The striking similarity of the calculated C═O stretching frequencies in the harmonic spectra of $\mathbf{IV}_{O(2)}$ and $\mathbf{X}_{O(2)/O(2)}$ suggests that addition of a second theophylline molecule to $\mathbf{IV}_{O(2)}$ to form $\mathbf{X}_{O(2)/O(2)}$ does not involve significant interaction between the theophylline molecules. The Na$^+$ effectively electrostatically anchors the groups at a long distance (4.28 Å), dramatically reducing anharmonicity as a result of minimizing interactions between the theophylline molecules. Finally, the average intensity of the calculated harmonic spectrum of $\mathbf{X}_{O(2)/O(2)}$ is approximately twice that of $\mathbf{IV}_{O(2)}$, which is intuitive since each $\mathbf{X}_{O(2)/O(2)}$ has twice as many theophylline molecules available to absorb IR radiation, relative to $\mathbf{IV}_{O(2)}$.

4. Conclusions

The gas phase IRMPD spectrum of the SCBD of theophylline has been obtained and characterized using energetic and spectral information provided by electronic structure calculations at the MP2(full)/aug-cc-pCVTZ[Na,N(9),O(2),O(6)]/6-

311+(2d,2p)//B3LYP/6-311+G(d,p) and B3LYP/6-311+G(d,p) levels of protocol, respectively.

The IRMPD spectrum and electronic structure calculations have shown the most stable isomer of the SCBD of theophylline exists as $\mathbf{X}_{O(2)/O(2)}$, a highly symmetric zero average dipole moment species, followed by isomers $\mathbf{IX}_{O(2)/O(6)}$ and $\mathbf{VIII}_{O(6)/O(6)}$, with calculated differences in relative free energies (298 K) of 10.9 and 11.6 kJ mol^{-1}, respectively at the MP2(full)/aug-cc-pCVTZ[Na,N(9),O(2),O(6)]/6-311+(2d,2p)//B3LYP/6-311+G(d,p) level of protocol. Considering the existence of thermalized ions under the experimental conditions and assuming that the IRMPD efficiency of $\mathbf{IX}_{O(2)/O(6)}$ is similar to $\mathbf{X}_{O(2)/O(2)}$ and $\mathbf{VIII}_{O(6)/O(6)}$, then the calculated free energies of SCBD formation (298 K) predict that a statistical distribution of $\mathbf{X}_{O(2)/O(2)}$ to $\mathbf{IX}_{O(2)/O(6)}$ and $\mathbf{VIII}_{O(6)/O(6)}$ should exist as approximately 81–1 and 108–1, respectively. The IRMPD spectrum shows no presence of SCBDs exhibiting inefficient (C(2/6)═O···Na$^+$···N(9)) or efficient (N(9)···Na$^+$···N(9)) nitrogen–Na$^+$ interactions, which is also consistent with the predictions of electronic structure calculations.

For $\mathbf{X}_{O(2)/O(2)}$, the large interatomic distance (4.28 Å) between the oxygen atoms on the C(2)═O···Na$^+$···O═C(2) axis provides sufficient separation of the theophylline molecules such that the effects of anharmonicity are significantly reduced relative to that observed for more tightly associated electrostatic ions, such as the PBD of theophylline and ammonia [4]. This is demonstrated by the match of the calculated vibrational signatures to $\mathbf{X}_{O(2)/O(2)}$ to that of the experimental IRMPD spectrum, with a MAD of the calculated harmonic and anharmonic frequencies of 11 and 28 cm^{-1}, respectively. It has also been shown computationally that the sodiated monomer ($\mathbf{IV}_{O(2)}$) possesses nearly identical C═O···Na$^+$ IR stretching signatures as $\mathbf{X}_{O(2)/O(2)}$, further supporting the conclusion that addition of a second theophylline molecule to $\mathbf{IV}_{O(2)}$, to form $\mathbf{X}_{O(2)/O(2)}$, does not significantly perturb the diagnostic IR frequencies of either theophylline molecule. The consequence of these observations is substantial due to the huge computational cost of performing anharmonic, rather than harmonic, analyses at the B3LYP/6-311+G(d,p) level of protocol, with the anharmonic and harmonic frequency calculations for $\mathbf{X}_{O(2)/O(2)}$ requiring 56 and 1.5 days, respectively.

Acknowledgements

The generous financial support by the Natural Sciences and Engineering Research Council of Canada (NSERC) is gratefully acknowledged as is the financial support of the European Commission through the NEST/ADENTURE program (EPITOPES, Project No. 15637). We are very grateful for the valuable assistance of the CLIO team, P. Maitre, J. Lemaire, J.M. Bakker, T. Besson, D. Scuderi and J.M. Ortega. and would also like to thank the CLIO technical support staff, for their outstanding assistance and kind hospitality during our stay in Orsay.

References

[1] B.G. Cosio, J.B. Soriano, Eur. Respir. J. 34 (2009) 5.
[2] M. Fukuda, S. Yuka, H. Hitomi, K. Kazuyo, M. Takehiko, I. Eiichi, Epilepsia 51 (2010) 483.
[3] E.E. Ferapontova, K.V. Gothelf, Langmuir 25 (2009) 4279.
[4] R.A. Marta, R. Wu, K.R. Eldridge, J.K. Martens, T.B. McMahon, Phys. Chem. Chem. Phys. 12 (2010) 3431.
[5] J.T. O'Brien, J.S. Prell, J.D. Steill, J. Oomens, E.R.J. Williams, Phys. Chem. A 112 (2008) 10823.
[6] C.G. Atkins, K. Rajabi, E.A.L. Gillis, T.D. Fridgen, J. Phys. Chem. A 112 (2008) 10220.
[7] O.P. Balaj, C. Kapota, J. Lemaire, G. Ohanessian, Int. J. Mass Spectrom. 269 (2008) 196.
[8] M.F. Bush, M.W. Forbes, R.A. Jockush, J. Oomens, N.C. Polfer, R.J. Saykally, E.R. Williams, J. Phys. Chem. A 111 (2007) 7753.
[9] M.F. Bush, J. Oomens, R.J. Saykally, E.R. Williams, J. Phys. Chem. A 112 (2008) 8578.
[10] D.R. Carl, T.E. Cooper, J. Oomens, J.D. Steill, P.B. Armentrout, Phys. Chem. Chem. Phys. 12 (2010) 3384.
[11] M.W. Forbes, M.F. Bush, N.C. Polfer, J. Oomens, R.C. Dunbar, E.R. Williams, R.A. Jockush, J. Phys. Chem. A 111 (2007) 11759.
[12] A.L. Heaton, V.N. Bowman, J. Oomens, J.D. Steill, P.B. Armentrout, J. Phys. Chem. A 113 (2009) 5519.
[13] C. Kapota, J. Lemaire, P. Maitre, G. Ohanessian, J. Am. Chem. Soc. 126 (2004) 1836.
[14] J.S. Prell, T.G. Flick, J. Oomens, G. Berden, E.R. Williams, J. Phys. Chem. A 114 (2010) 854.
[15] P.B. Armentrout, M.T. Rodgers, J. Oomens, J.D. Steill, J. Phys. Chem. A 112 (2008) 2248.
[16] M.T. Rodgers, P.B. Armentrout, J. Oomens, J.D. Steill, J. Phys. Chem. A 112 (2008) 2258.
[17] E.B. Cagmat, J. Szczepanski, W.L. Pearson, D.H. Powell, J.R. Eyler, N.C. Polfer, Phys. Chem. Chem. Phys. 12 (2010) 3474.
[18] D.T. Moore, J. Oomens, J.R. Eyler, G. von Helden, G. Meijer, R.C. Dunbar, J. Am. Chem. Soc. 127 (2005) 7243.
[19] J. Szczepanski, H.Y. Wang, M. Vala, A. Tielens, J.R. Eyler, J. Oomens, Astrophys. J. 646 (2006) 666.
[20] J.J. Valle, J.R. Eyler, J. Oomens, D.T. Moore, A.F.G. van der Meer, G. von Helden, G. Meijer, C.L. Hendrickson, A.G. Marshall, G.T. Blakney, Rev. Sci. Instrum. 76 (2005) 023103–023111.
[21] R.P. Dain, C.M. Leavitt, J. Oomens, J.D. Steill, G.S. Groenewold, M. Van Stipdonk, J. Rapid Commun. Mass Spetrom. 24 (2010) 232.
[22] G.S. Groenewold, C.M. Leavitt, R.P. Dain, J. Oomens, J.D. Steill, M. van Stipdonk, J. Rapid Commun. Mass Spetrom. 23 (2009) 2706.
[23] C.M. Leavitt, J. Oomens, R.P. Dain, J. Steill, G.S. Groenewold, M.J. Van Stipdonk, J. Am. Soc. Mass Spectrom. 20 (2009) 772.
[24] R.C. Dunbar, A.C. Hopkinson, J. Oomens, C.K. Siu, K.W.M. Siu, J.D. Steill, U.H. Verkerk, J.F. Zhao, J. Phys. Chem. B 113 (2009) 10403.
[25] R.C. Dunbar, N.C. Polfer, J. Oomens, J. Am. Chem. Soc. 129 (2007) 14562.
[26] R.C. Dunbar, J.D. Steill, N.C. Polfer, J. Oomens, J. Phys. Chem. B 113 (2009) 10552.
[27] R.C. Dunbar, J.D. Steill, N.C. Polfer, J. Oomens, J. Phys. Chem. A 113 (2009) 845.
[28] A.L. Heaton, R.M. Moision, P.B. Armentrout, J. Phys. Chem. A 112 (2008) 3319.
[29] K. Hiraoka, H. Takimoto, J. Phys. Chem. 90 (1986) 5910.
[30] S. Hoyau, K. Norrman, T.B. McMahon, G. Ohanessian, J. Am. Chem. Soc. 121 (1999) 8864.
[31] P. Wang, M.J. Polce, G. Ohanessian, C. Wesdemiotis, J. Mass Spectrom. 43 (2008) 485.
[32] S.D.M. Chinthaka, Y. Chu, N.S. Rannulu, M.T. Rodgers, J. Phys. Chem. A 110 (2006).
[33] M.T. Rodgers, P.B. Armentrout, Acc. Chem. Res. 37 (2004) 989.
[34] C.H. Ruan, M.T. Rodgers, J. Am. Chem. Soc. 126 (2004) 14600.
[35] R. Amunugama, M.T. Rodgers, Int. J. Mass Spectrom. 227 (2003) 339.
[36] R. Amunugama, M.T. Rodgers, Int. J. Mass Spectrom. 227 (2003) 1.
[37] R. Amunugama, M.T. Rodgers, Int. J. Mass Spectrom. 222 (2003) 431.
[38] R. Amunugama, M.T. Rodgers, J. Phys. Chem. A 106 (2002) 9718.
[39] R. Amunugama, M.T. Rodgers, J. Phys. Chem. A 106 (2002) 9092.
[40] R. Amunugama, M.T. Rodgers, J. Phys. Chem. A 106 (2002) 5529.
[41] H. Huang, M.T. Rodgers, J. Phys. Chem. A 106 (2002) 4277.
[42] P. Wang, C. Wesdemiotis, C. Kapota, G. Ohanessian, J. Am. Soc. Mass Spectrom. 18 (2007) 541.
[43] M.M. Kish, G. Ohanessian, C. Wesdemiotis, Int. J. Mass Spectrom. 227 (2003) 509.
[44] M.M. Kish, C. Wesdemiotis, G. Ohanessian, J. Phys. Chem. B 108 (2004) 3086.
[45] P.B. Armentrout, A. Babriel, R.M. Moision, Int. J. Mass Spectrom. 283 (2009) 56.
[46] N.C. Polfer, J. Oomens, R.C. Dunbar, Chem. Phys. Chem. 9 (2008) 579.
[47] J. Lemaire, P. Boissel, M. Heninger, G. Mauclaire, G. Bellec, H. Mestdagh, A. Simon, S.L. Caer, J.M. Ortega, F. Glotin, P. Maitre, Phys. Rev. Lett. 89 (2002) 273002–273011.
[48] P. Maitre, S. Le Caer, A. Simon, W. Jones, J. Lemaire, H.N. Mestdagh, M. Heninger, G. Mauclaire, P. Boissel, R. Prazeres, F. Glotin, J.M. Ortega, Nucl. Instrum. Methods Phys. Res., Sect. A 507 (2003) 541.
[49] R. Wu, T.B. McMahon, J. Mass Spectrom. 43 (2008) 1641.
[50] M.J. Frisch, G.W. Trucks, H.B. Schlegel, G.E. Scuseria, M.A. Robb, J.R. Cheeseman, G. Scalmani, V. Barone, B. Mennucci, G.A. Petersson, H. Nakatsuji, M. Caricato, X. Li, H.P. Hratchian, A.F. Izmaylov, J. Bloino, G. Zheng, J.L. Sonnenberg, M. Hada, M. Ehara, K. Toyota, R. Fukuda, J. Hasegawa, M. Ishida, T. Nakajima, Y. Honda, O. Kitao, H. Nakai, T. Vreven, J.A. Montgomery Jr, J.E. Peralata, F. Ogliaro, M. Bearpark, J.J. Heyd, E. Brothers, K.N. Kudin, V.N. Staroverov, R. Kobayashi, J. Normand, K. Raghavachari, A. Rendell, J.C. Burant, S.S. Iyengar, J. Tomasi, M. Cossi, N. Rega, J.M. Millam, M. Klene, J.E. Knox, J.B. Cross, V. Bakken, C. Adamo, J. Jaramillo, R. Gomperts, R.E. Stratmann, O. Yazyev, A.J. Austin, R. Cammi, C. Pomelli, J.W. Ochterski, R.L. Martin, K. Morokuma, V.G. Zakrzewski, G.A. Voth, P. Salvador, J.J. Dannenberg, S. Dapprich, A.D. Daniels, O. Farkas, J.B. Foresman, J.V. Ortiz, J. Cioslowski, D.J. Fox, Gaussian 09, Revision A.02, Gaussian, Inc., Wallingford, CT, 2009.
[51] A. Gil, S. Simon, L. Rodriguez-Santiago, J. Bertran, M. Sodupe, J. Chem. Theory Comput. 3 (2007) 2210.
[52] M. Leopoldini, I.P. Pitarch, N. Russo, M. Toscano, J. Phys. Chem. A 108 (2004) 92.
[53] R.J. Nieckarz, N. Oldridge, T.B. McMahon, Int. J. Mass Spectrom. 267 (2007) 338.
[54] I.A. Topol, S.K. Burt, N. Russo, M. Toscano, J. Am. Soc. Mass Spectrom. 10 (1999) 318.

[55] R. Wu, T.B. McMahon, J. Am. Chem. Soc. 129 (2007) 11312.
[56] R.A. Marta, T.D. Fridgen, T.B. McMahon, J. Phys. Chem. A 111 (2007) 8792.
[57] M.P. Andersson, P. Uvdal, J. Phys. Chem. A 109 (2005) 2937.
[58] V. Barone, J. Chem. Phys. 120 (2004) 3059.
[59] C.W. Bauschlicher Jr, H. Partridge, J. Chem. Phys. 103 (1995) 1788.
[60] I. Bytheway, M.W. Wong, Chem. Phys. Lett. 282 (1998) 219.
[61] C.F. Correia, C. Clavaguera, U. Erlekam, D. Scuderi, G. Ohanessian, Chem. Phys. Chem. 9 (2008) 2564.
[62] M.D. Halls, J. Velovski, B.H. Schlegel, Theor. Chem. Acc. 105 (2001) 413.
[63] J. Jaramillo, G.E. Scuseria, Chem. Phys. Lett. 312 (1999) 269.
[64] B.G. Johnson, M.W. Gill, J.A. Pople, J. Chem. Phys. 98 (1993) 5612.
[65] A.P. Scott, L. Radom, J. Phys. Chem. 100 (1996) 16502.
[66] D. Scuderi, C.F. Correia, O.P. Balaj, G. Ohanessian, J. Lemaire, P. Maitre, Chem. Phys. Chem. 10 (2009) 1630.
[67] C.W. Bauschlicher Jr, S.R. Langhoff, H. Partridge, J.E. Rice, A. Komornicki, J. Chem. Phys. 95 (1991) 5142.
[68] D. Feller, E.D. Glendening, D.E. Woon, J. Chem. Phys. 193 (1995) 3526.
[69] K.A. Peterson, T.H. Dunning Jr., J. Chem. Phys. 117 (2002) 10548.
[70] K.A. Peterson, A.K. Wilson, D.E. Woon, T.H. Dunning Jr., Theor. Chem. Acc. 97 (1997) 251.